Dr. L. M. Hobbs
THE UNIVERSITY OF CHICAGO
YERKES OBSERVATORY
P.O. Box 258
WILLIAMS BAY, WI 53191-0258

P-17

THE INTERSTELLAR D_1 LINE AT HIGH RESOLUTION

L. M. Hobbs [1] and D. E. Welty [1]

University of Chicago

[1] Guest Observer, McDonald Observatory, University of Texas.

ABSTRACT

Observations at a resolving power $R = \lambda/\Delta\lambda = 5 \times 10^5$ or a velocity resolution $\Delta v = 0.6$ km s^{-1} are reported of the interstellar D_1 line of Na I in the spectra of γ Cas, δ Ori, ϵ Ori, π Sco, δ Cyg, and α Cyg. An echelle grating was used in a double-pass configuration with a CCD detector in the coude spectrograph of the 2.7m reflector at McDonald Observatory. At least 42 kinematically distinct clouds are detected along the light paths to the five more distant stars, in addition to a single cloud seen toward δ Cyg. The absorption lines arising in 13 of the clouds are sufficiently narrow and unblended to reveal clearly resolved hyperfine structure components split by 1.05 km s^{-1}. An additional 13 clouds apparently show comparably narrow, but more strongly blended, lines. For each individual cloud, upper limits T_{max} and $(v_t)_{max}$ on the temperature and the turbulent velocity, respectively, are derived by fitting the observed lines with theoretical absorption profiles. Twenty-three of the 43 clouds show $T_{max} < 450$ K and $\sqrt{3} \times (v_t)_{max} < 0.70$ km s^{-1}, the sound speed which corresponds to T = 80 K. The most stringent upper limits obtained for any of the clouds, from unblended lines, are $T_{max} < 160$ K and $(v_t)_{max} < 0.24$ km s^{-1}.

Subject Headings: interstellar: matter -- line profiles -- hyperfine structure

I. INTRODUCTION

Observations of the generally multiple components of an interstellar absorption line at a spectral resolution near the fundamental limit set by the thermal widths of the individual line components can provide two valuable advantages in studying the absorbing gas. Firstly, a nearly full enumeration of the various kinematically distinct parcels of gas along the observed light path is realized, within the unavoidable limits set by any negligible differences between the radial velocities of spatially separate gas clouds and by the minimum column density which corresponds to the threshhold for detection of the line. Secondly, accurate measurements can be made of the widths of the resolved line components, and hence of upper limits on the temperature and on the internal mass motions of each distinct cloud. Such rigorous temperature limits have hitherto been particularly difficult to obtain for most single interstellar clouds.

The potential utility of the readily accessible D lines of Na I for such purposes was pointed out by Hobbs (1969b), who emphasized that the splitting, $\Delta v = 1.05$ km s^{-1}, of the two s-resolved hyperfine structure components exceeds the thermal line width at $T \approx 80$ K by a factor of almost three. An instrumental resolving power of $R = \lambda/\Delta\lambda \geq 5 \times 10^5$, or a resolution of $\Delta\lambda \leq 12$ mÅ or $\Delta v \leq 0.6$ km s^{-1}, therefore will partially resolve a thermally broadened pair of hfs components formed in a cloud with $T \leq 500$ K, thereby immediately revealing a conspicuous signature of cold gas. The first successful observational detection of the resolved hfs components of the interstellar D lines was achieved with a Michelson interferometer by Blades, Wynne-Jones, and Wayte (1980; hereafter BWW), in four clouds along the light paths to δ Cyg and α Cyg. Those authors deduced temperature upper limits which averaged 260 K for the clouds in question, and they also showed that the turbulence in these clouds must be subsonic. More recently, Pettini (1988) obtained spectra of SN 1987a near its peak brightness and similarly identified several cold clouds showing resolved hfs components along that light path.

Since 1987, we have been conducting a somewhat wider survey of the interstellar D_1 line in the spectra of bright stars at distances $d \leq 500$ pc, recorded at a resolving power $R \approx 5 \times 10^5$. The survey, which is still in progress, currently extends to more than 30 bright stars; the illustrative results for six of those stars are reported here.

II. OBSERVATIONS

The spectra were obtained with the coude spectrograph of the 2.7 m telescope at McDonald Observatory, beginning in June 1987. The echelle grating was used in the double-pass configuration, with the 800 x 800 TI-2 CCD detector placed at the "scanner" focus and with grating C used for cross dispersion (Tull 1972). The resulting reciprocal dispersion at the D_1 line is 0.10 Å mm^{-1}, or 0.15 km

s^{-1} per two pixels of the detector, each pixel being 15 μm wide. This very high dispersion is produced by a camera mirror with a focal length of 8.05 m, which is also identically the collimator mirror in this Littrow configuration. A 90 μm entrance slit, which corresponded to 0.21 arcsec on the sky, was used for nearly all of the spectra reported here. This choice yielded an actual instrumental resolution (FWHM) of $\Delta v = 0.6 \pm 0.1$ km s^{-1}, or a resolving power $R = 5 \times 10^5$, as deduced from the profiles of the lines measured in the various comparison lamp spectra noted below. The two-pixel binning of the CCD along the dispersion thus yielded a data format oversampled by approximately a factor of two. The various exposure times were strongly governed by the seeing; in 2 arcsec seeing, a signal-to-noise ratio S/N ≈ 120 was achieved for ε Ori (V = 1.70) in about 30 minutes.

The observed profile of the interstellar D_1 line is shown in Figure 1 for each of six stars; relevant data for the stars are collected for reference in Table 1 (Hobbs 1969a; Hobbs 1976; Hoffleit 1982). The results derived from the spectra will be discussed in § III. At least 13 examples of resolved hfs components are immediately apparent in the spectra; the pertinent line pairs are split by 1.05 km s^{-1}, and the strength of the component at the longer wavelength is greater by a factor 5/3, in the optically thin limit. Except for δ Ori, the data shown are the respective averages of two separate exposures, which in each case showed good mutual agreement. The spacing between data points in the individual exposures corresponded to 0.15 km s^{-1}; these individual exposures were interpolated onto standardized velocity grids having points spaced by 0.1 km s^{-1} and then were respectively added. In each of these summed spectra, adjacent pairs of such points were added to yield the final, average spectra shown, which consist of data points spaced by 0.2 km s^{-1}. For all six stars, these final spectra in Figure 1 show $120 \lesssim S/N \lesssim 170$.

Owing to the spectrograph's high dispersion, the useful spectral interval included in a single exposure at the D lines was only 1.2 Å, or 60 km s^{-1}. All observations made so far were recorded at the D_1 line, rather than the D_2 line, in order to minimize both line saturation and interference from telluric lines. The relatively few telluric lines originally present in our spectra did not overlap with any of the interstellar lines and have been removed through division of the relevant region of each program-star spectrum by a Gaussian line profile which was empirically fitted to the telluric absorption.

Because the interstellar absorption toward each of δ Ori, ε Ori, and α Cyg spans about half of the 60 km s^{-1} range recorded in a single exposure, an uncertainty exists in each of these three cases in correctly interpolating the continuum across the regions of absorption. This uncertainty is largest for α Cyg, which, at a spectral type of A2 Ia, also shows a strong, fairly narrow, stellar D_1 line. This stellar line has been empirically fitted by a polynomial curve and removed from the data in Figure 1. For the simpler cases of δ Ori and ε Ori, such continuum placement errors probably amount to no more than 4% of the continuum intensity.

The double-pass configuration of the spectrograph effectively suppresses all scattered light (Tull 1972). The principal error in determining the true zero-point for residual intensities therefore arises in subtracting the background levels recorded by the CCD detector. After the one echelle order which falls on the detector was flat-fielded, the "one-dimensional" spectrum was extracted using the IRAF apextract routines. The background spectrum was estimated by fitting at each wavelength point the background recorded on either side of the stellar spectrum; a smoothed version of that background spectrum was then subtracted, to obtain the corrected stellar spectrum. Except possibly for α Cyg, the final uncertainty in the intensity zero-point should not exceed 2% of the continuum intensity, in each of the spectra in Figure 1.

Accurate wavelength scales were determined from the D_1 line emitted by a Na/Ne hollow cathode lamp and from the comparison spectrum provided by an iodine absorption cell illuminated by a tungsten-filament lamp. The I_2 spectrum is quite rich near the D_1 line (Gerstenkorn and Luc 1978; 1979). The instrumental resolution (FWHM) of $\Delta v = 0.6 \pm 0.1$ km s^{-1} cited above was determined empirically by comparing the measured profiles of various I_2 lines, the D_1 line from the Na/Ne lamp, the Th I λ5760.551 line from a Th/Ne lamp, and the λ6328 line of a He-Ne laser. In the latter two cases, the spectrograph was tuned to the adjacent wavelengths by making small adjustments to the setup at the D_1 line.

A more complete description of the calibration and data-reduction procedures will be given in a subsequent account of the full observational program.

III. RESULTS

The method of profile fitting has been used to determine the radial velocity, the line-width parameter b, and the column density N(Na I) for each distinct absorbing cloud along each light path (Hobbs 1969b; Vidal-Madjar et al 1977; Welty, Hobbs, and York 1990). A Maxwellian form was assumed for the distribution of the radial velocities within each cloud, and, in order to fit the observed spectra, the resulting theoretical profiles were convolved with a Gaussian instrumental function having a FWHM of $\Delta\lambda$ = 12 mÅ, or Δv = 0.6 km s^{-1}. Because the excitation energy of the upper hfs level of the ground $^2S_{1/2}$ level is equivalent to $T = \Delta E/k = 0.085$ K, the ratio of the populations of the upper F = 2 level and the lower F = 1 level was always set equal to 5/3, the corresponding ratio of the statistical weights. The corresponding hfs transition at 16.9 cm, which is analogous to the 21-cm line of H I, has not yet been detected in atomic or molecular interstellar clouds (Turner 1987).

The results of fitting such theoretical profiles to the observations of the six program stars

are given in Figure 1 and Table 2. The number of clouds assumed in fitting each spectrum was restricted to the minimum possible value which permitted all of the various components unambiguously present in the data to be accounted for. The upper limits T_{max} on the respective cloud temperatures given in Table 2 were calculated from the relation $T_{max} = (m/2k)b^2$, in the limit of exclusively thermal broadening of the line. In the alternative limit of a gas at T = 0, upper limits $(v_t)_{max}$ on the respective "turbulent" velocities within the clouds were similarly calculated from the relation $(v_t)_{max} = b/\sqrt{2}$, which obtains under the assumption of a Gaussian spectrum of turbulent velocities which have an rms value v_t for the radial components of the velocities. In general, $b^2 = 2v_t^2 + (2kT/m)$, so that the actual values of both T and v_t in any cloud are almost always simultaneously smaller than the alternative limiting values given in Table 2. The values of T_{max} and $(v_t)_{max}$ necessarily refer to the relatively dense, cool regions of each cloud, into which the Na I atoms are expected to be concentrated preferentially.

Partially resolved hfs components are apparent for 13 cool clouds whose lines happen to be sufficiently unblended with those of other clouds to preserve this signature of cold gas. In all 13 cases, which are indicated in Table 2 (see footnote), the derived line widths are characterized by $b \leq 0.6$ km s^{-1}, as is to be expected. An additional 13 clouds, whose lines are more severely blended with those of other clouds which in nearly all cases have larger Na I column densities, also show line widths which satisfy the same criterion. A prototype of this group is cloud 7 seen toward δ Ori, with b = 0.33 km s^{-1} or T_{max} = 150 K. This cloud shows only the longer-wavelength, stronger hfs component in a nearly unblended, and quite narrow, form. Thus, apart from the effects of blending, at least 26 of these 43 clouds would show resolved hfs components, at our resolution. Consequently, this signature is apparently the normal one for diffuse interstellar clouds.

The spectra in Figure 1 and the derived cloud parameters in Table 2 generally agree with the results obtained in two previous, related investigations. Either or both of the D lines in the spectra of all six stars were previously observed by Hobbs (1969a; 1976), using the interferometric PEPSIOS scanner at a lower effective resolving power. Apart from some small differences in the residual intensities which presumably arise from differences in continuum placement or errors in background subtraction in either set of spectra, the overall agreement between them is excellent. The obviously superior resolution of the new spectrum constitutes the critical difference between the two. For δ Cyg and α Cyg, the profiles of both D lines were also measured previously by BWW at a resolving power R = 6×10^5, approximately 20% higher than that selected in the present survey. Our results show good agreeement with their data at the D_1 line. In particular, the values of b and N(Na I) derived for the only

cloud detected along the light path to the nearby star δ Cyg disagree in the two investigations by only 11% and 16%, respectively. For α Cyg, BWW derived a nine-cloud fit to the D lines which is similar, in all of its major features, to our ten-cloud result for the same velocity interval, $-25 \leq v \leq +3$ km s^{-1} (Table 2). Some differences exist with respect to line components which are either strongly blended or intrinsically quite weak; in both circumstances, the inferred parameters of the absorbing clouds are necessarily less certain, in both studies.

These very narrow, apparently non-variable lines which appear in the spectra of bright stars may have some future value as radial velocity standards (Welty, Hobbs, and York 1990). A comparison of the absolute radial velocities listed in Table 2 with those found in the two previous studies therefore deserves some comment. The present velocities can be compared first with the earlier PEPSIOS results for the five program stars other than α Cyg. For these five stars, there is an apparent systematic zero-point offset of -0.5 ± 0.2 km s^{-1} (new minus PEPSIOS). After these systematic offsets are removed, the random velocity differences among the many line components in the five pairs of spectra show an rms scatter smaller than ± 0.2 km s^{-1}, although the difference in instrumental resolutions makes an exact value difficult to estimate. In contrast, a difference of about 2.5% exists between the overall velocity scales in the two specta of α Cyg, an unexplained difference which probably cannot be accounted for by the presence of a strong stellar line. An additional comparison of our absolute velocities with those of BWW for two stars in common gives the following results. For the single cloud seen toward δ Cyg, and for the relatively unblended lines toward α Cyg, the zero points for the radial velocities agree essentially exactly, while the additional random errors are again smaller than ± 0.2 km s^{-1}. In summary, except for the PEPSIOS scan of α Cyg, the absolute velocities in all three sets of data are typically accurate to ± 0.5 km s^{-1} or better. An analysis, now in progress, of the full set of data available in our present survey may further clarify this question.

IV. DISCUSSION

We anticipate that the most useful results of these observations will be the rigorous upper limits $(v_t)_{max}$ and, especially, T_{max} eventually to be derived for a large number of single interstellar clouds. These limits should be valuable in future, intensive "case studies" of various individual clouds. Of the 43 values of T_{max} in Table 2, the lowest is $T_{max} = 75$ K, seven occupy the domain $T_{max} \leq 200$ K, and 26 show $T_{max} \leq 600$ K. The most stringent upper limit obtained from unblended lines is $T_{max} < 160$ K (ε Ori, cloud 1 and α Cyg, cloud 10). The actual temperatures presumably are often appreciably lower than these already fairly stringent upper limits. There are also six values $T_{max} \geq 2850$ K, which reveal

gas that may be much warmer and/or more turbulent than most of the interstellar material which absorbs effectively at the D lines. Because Na I is formed primarily by radiative recombination in interstellar gas, there is a strong, inherent selection effect against the detection of relatively warm, low-density gas by means of Na I lines. Only one component in the spectra of these six stars (γ Cas, cloud 1) apparently is broad enough to allow the possibility that it arises in predominantly ionized gas.

Several other important features of the temperatures deduced here should also be pointed out. The FWHM of an individual, thermally broadened hfs component formed in gas at $T < 200$ K is $\Delta v < 0.63$ km s^{-1}. Because the instrumental resolution (FWHM) of our survey is also 0.6 ± 0.1 km s^{-1} (§ II), the instrumental broadening of the observed profiles therefore will make reliable measurement of the temperatures progressively more difficult at $T \lesssim 200$ K, where the intrinsic thermal line widths become increasingly narrower than the instrumental width. A histogram of even this preliminary portion of the survey illustrates this effect (Figure 2), because the typical temperature of most neutral interstellar gas probably is $T \approx 80$ K (Spitzer 1978). The general increase in the number of clouds as T_{max} decreases below 1200 K is in fact reversed here at $T < 200$ K, owing to the effects of instrumental broadening. On the other hand, some of the broader line components could in fact consist of two or more, narrower, blended components which arise in spatially separate clouds with similar radial velocities. The total number of clouds identified in Table 2 therefore is only a lower limit, and even the small numbers of clouds with relatively large values of T_{max} may also be overestimated.

Among the 43 values of $(v_t)_{max}$ listed in Table 2, twenty-three provide upper limits $(v_t)_{max} < 0.4$ km s^{-1}, or corresponding three-dimensional limits $\sqrt{3} \times (v_t)_{max} \leq 0.7$ km s^{-1}, the value of the isothermal sound speed at $T = 80$ K. Thus, if the actual temperature of the clouds along these six light paths typically is $T \approx 80$ K, more than half of the clouds do indeed show turbulence or internal mass motions which are demonstrably subsonic, in agreement with the conclusion reached previously by BWW. If a standard thermal broadening appropriate to $T = 80$ K is conservatively assumed and is additionally taken into account, by calculating $\sqrt{3} \times v_t = \{ 3[b^2 - (2kT/m)]/2 \}^{1/2}$ with $T = 80$ K, then three additional clouds show $\sqrt{3} \times v_t \leq 0.7$ km s^{-1}.

It is a pleasure to acknowledge the hospitality of the staff at McDonald Observatory and, in particular, the expert help of David Doss in critically aligning the coude spectrograph. Ed Jenkins and Chuck Joseph provided data from the UV spectrum of π Sco in advance of publication, and Craig J. Sansonetti supplied information about the molecular iodine spectrum. Bryan Penprase assisted with some of the observations. Finally, we are grateful to the National Aeronautics and Space Administration for

financial support of this work, through grant NAGW-1475 to the University of Chicago.

TABLE 1

Stellar Data

star	V	Sp	RV (km s^{-1})	v sin i (km s^{-1})	d (pc)	E(B-V)
γ Cas	2.2v	B0.5 IVp	-7	300:	210:	--
δ Ori	2.20	09.5 II	16v	152	450	0.09
ϵ Ori	1.70	B0 Ia	26	87	450	0.05
π Sco	2.88	B1 V	-3v	100:	170	0.07
δ Cyg	2.92	B9.5 III	-21	149	50	0.00
α Cyg	1.26	A2 Ia	-5v	21	500	0.09

TABLE 2

Cloud Properties

star	cloud	v ($km\ s^{-1}$)	b ($km\ s^{-1}$)	N(Na I) ($10^{10}\ cm^{-2}$)	T_{max} (K)	$(v_t)_{max}$ ($km\ s^{-1}$)
γ Cas	1	-7.2	2.60	27.5	9,340	1.84
	2[a]	-5.1	0.59	16.1	480	0.42
	3	-3.75	0.23	3.1	75	0.16
	4[a]	-2.8	0.40	10.3	220	0.28
	5	-1.0	1.26	1.6	2,190	0.89
δ Ori	1	5.5	1.65	1.6	3,760	1.17
	2	9.3	1.90	6.0	4,990	1.34
	3	15.1	0.91	2.6	1,140	0.64
	4	21.8	1.30	10.1	2,340	0.92
	5	24.5	1.10	15.8	1,670	0.78
	6[a]	25.3	0.43	7.5	255	0.30
	7	26.6	0.33	4.6	150	0.23
ϵ Ori	1[a]	3.0	0.34	7.9	160	0.24
	2	5.0	1.30	4.7	2,340	0.92
	3	8.6	1.50	5.0	3,110	1.06
	4	11.0	0.77	33.8	820	0.54
	5	12.5	0.46	13.0	290	0.33
	6[a]	14.8	0.47	5.8	305	0.33
	7[a]	17.3	0.50	18.0	345	0.35
	8	22.8	0.52	13.0	375	0.37
	9	23.95	0.54	13.6	405	0.38
	10[a]	24.9	0.48	49.6	320	0.34
	11	26.0	0.89	21.3	1,090	0.63
	12	28.1	0.79	7.5	865	0.56

π Sco	1	-22.2	1.03	2.9	1,470	0.73
	2	-17.3	1.50	14.3	3,110	1.06
	3[a]	-15.9	0.50	14.8	345	0.35
	4	-14.9	0.35	5.6	170	0.25
	5	-14.1	0.58	3.5	465	0.41
	6[a]	-12.6	0.48	4.5	320	0.34
	7	-7.15	0.91	2.6	1,140	0.64
δ Cyg	1[a]	-18.6	0.40	29.5	220	0.28
∝ Cyg	1	-21.9	0.57	150.	450	0.40
	2	-20.8	0.28	23.7	110	0.20
	3	-13.3	0.53	120.	390	0.37
	4	-12.0	0.73	49.0	735	0.52
	5	-9.5	0.44	40.3	270	0.31
	6[a]	-8.2	0.58	66.3	465	0.41
	7	-6.0	1.44	26.0	2,870	1.02
	8	-3.9	0.42	12.9	245	0.30
	9[a]	-2.8	0.37	29.1	190	0.26
	10[a]	1.3	0.34	30.3	160	0.24
	11	5.5	0.41	0.8	230	0.29

[a] Partially resolved hfs components are clearly evident, for a cool cloud whose lines are not seriously blended with those of another cloud.

REFERENCES

Blades, J. C., Wynne-Jones, I., and Wayte, R. 1980, M.N.R.A.S. 193, 849 (BWW).

Gerstenkorn, S., and Luc, P. 1978, Atlas du spectre d'absorption de la molecule de l'iode entre 14,800 - 20,000 cm^{-1} (Editions du C.N.R.S., 15, Paris)

---------- 1979, Rev. de Physique Appliquee 14, 791.

Hobbs, L. M. 1969a, Ap. J. 157, 135.

Hobbs, L. M. 1969b, Ap. J. 157, 165.

Hobbs, L. M. 1976, Ap. J. 203, 143.

Hoffleit, D. 1982, The Bright Star Catalogue (4th ed.; New Haven: Yale University Observatory).

Jenkins, E. B., Lees, J. F., van Dishoeck, E., and Wilcots, E. M. 1989, Ap. J. 343, 785.

Joseph, C. L., and Jenkins, E. B. 1990, Ap. J. (submitted).

Pettini, M. 1988, Proc. Astr. Soc. Australia 7, 527.

Spitzer, L. 1978, Physical Processes in the Interstellar Medium (New York: Wiley-Interscience).

Tull, R. G. 1972, Proceedings ESO/CERN Conference on Auxiliary Instrumentation for Large Telescopes (Geneva: European Southern Observatory), p. 259.

Turner, B. E. 1987, Ap. J. 314, 363.

Vidal-Madjar, A., Laurent, C., Bonnet, R. M., and York, D. G. 1977, Ap. J. 211, 91.

Welty, D. E., Hobbs, L. M., and York, D. G. 1990, Ap. J. Suppl. (in press).

FIGURE CAPTIONS

Fig. 1. The interstellar D_1 line in the spectra of six stars. The plus signs constitute the observational data, and the solid curves are the theoretical profiles which have been fitted to the data (§ III). In the cases of δ Ori and δ Cyg, the theoretical profiles are omitted, to allow an unimpeded view of the data. The tick marks above the continua indicate the stronger of the two s-resolved hfs omponents arising in the various clouds. The radial velocity scales also refer to this component, which falls at the longer wavelength of the pair. To locate the correct position for the weaker component, the hfs splitting of 1.05 km s^{-1} must therefore be subtracted from the velocities shown by the tick marks. For observations of many interstellar lines in the ultraviolet spectrum of π Sco at a resolution $\Delta v \approx 2$ km s^{-1}, see Jenkins et al (1989) and Joseph and Jenkins (1990).

Fig. 2. A histogram of the upper limits, T_{max}, on the temperatures of 37 interstellar clouds. Six clouds with $2{,}400 < T_{max} \leq 9{,}400$ K are not included.

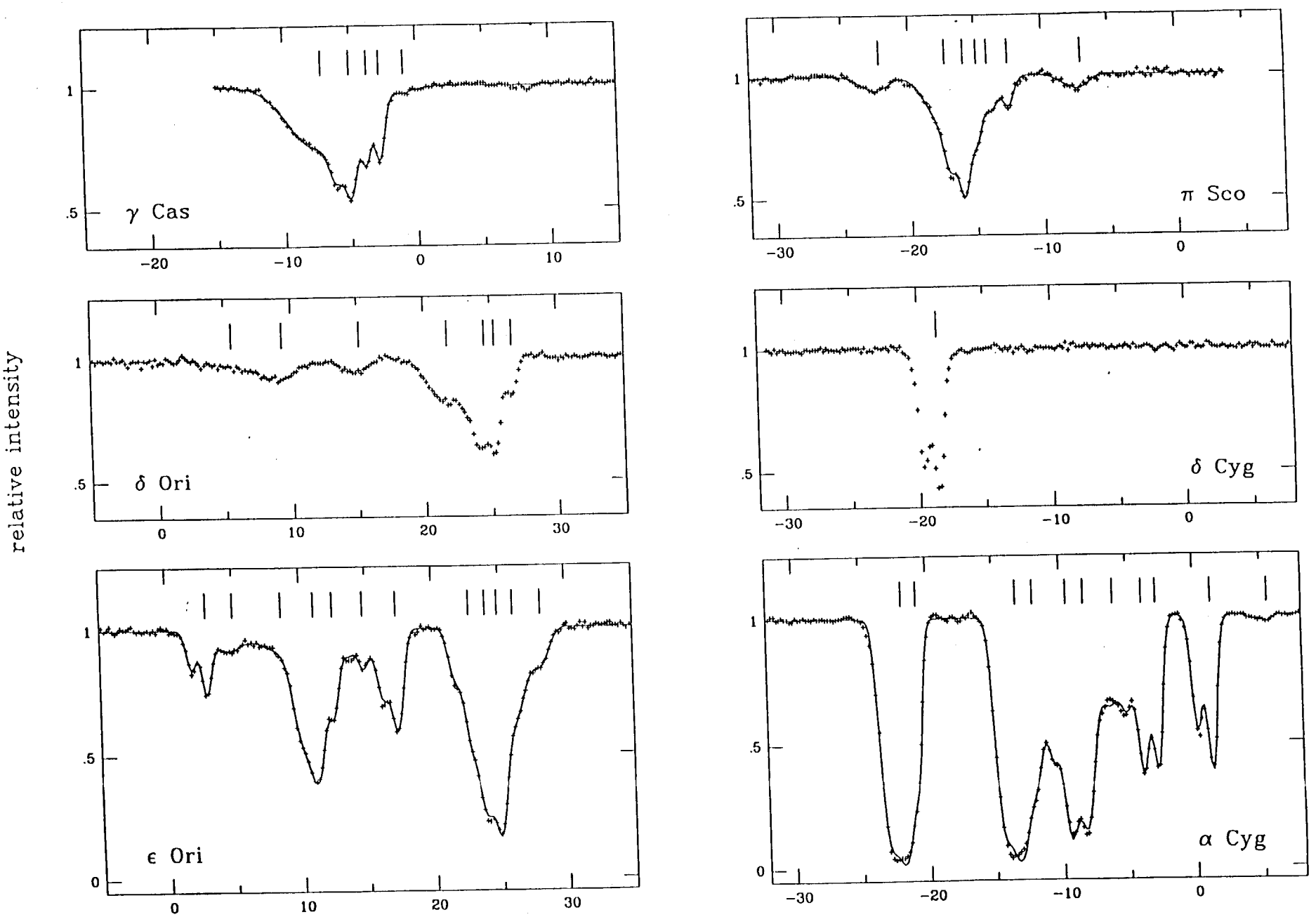
γ Cas
δ Ori
ϵ Ori
π Sco
δ Cyg
α Cyg
relative intensity
heliocentric radial velocity (km/s)

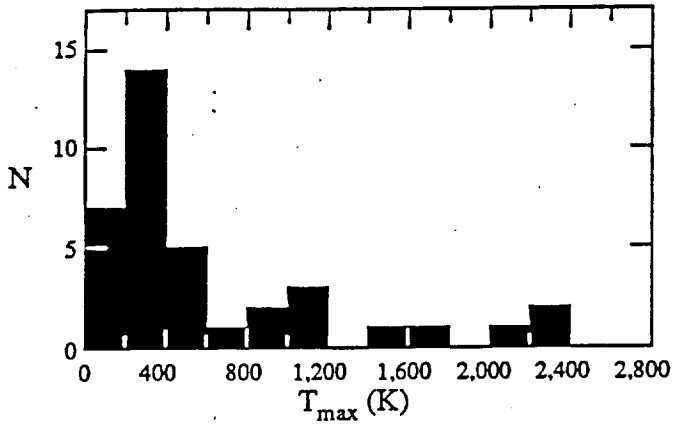
15
10
5
0
N
0
400
800
1,200
1,600
2,000
2,400
2,800
T_{max} (K)

L. M. Hobbs
Yerkes Observatory
University of Chicago
Williams Bay, WI 53191-0258

D. E. Welty
Astronomy and Astrophysics Center
University of Chicago
5640 S. Ellis Ave.
Chicago, IL 60637